Controlling Ion Transport through Multilayer Polyelectrolyte Membranes by Derivatization with Photolabile Functional Groups

Jinhua Dai, Anagi M. Balachandra, Jong Il Lee, and Merlin L. Bruening*

Department of Chemistry and Center for Fundamental Materials Research, Michigan State University, East Lansing, Michigan 48824

Received September 17, 2001; Revised Manuscript Received January 15, 2002

ABSTRACT: Increasing the net fixed-charge density in multilayer polyelectrolyte membranes using postdeposition reactions results in large enhancements of ion-transport selectivity. To control the fixed-charge density in poly(acrylic acid)/poly(allylamine hydrochloride) (PAA/PAH) films, we partially derivatized PAA using 2-nitrobenzyl bromide. The underivatized $-COO^-$ groups still allow adsorption of PAA/PAH membranes on a permeable support, while postdeposition UV irradiation of these films cleaves the 2-nitrobenzyl esters to form fixed-charge sites. Diffusion dialysis experiments show that PAA/PAH membranes prepared with 23%, 50%, and 65% 2-nitrobenzyl esterified PAA exhibit Cl^-/SO_4^{2-} selectivities of 100, 150, and 170, respectively (after photolysis). Underivatized PAA/PAH membranes show a selectivity of only 10. The order of magnitude increase in selectivity resulting from derivatization occurs with a minimal decrease in Cl^- flux. By modifying PAH with photolabile 2-nitrobenzyloxycarbonyl groups, we also introduced net, fixed positive charge into PAA/PAH films and improved cation (Na^+/Mg^{2+}) selectivity. Transport simulations suggest that both Donnan exclusion and selective diffusion contribute to selectivity.

Introduction

Membrane-based separations are attractive because of their operational simplicity and low energy costs, but limitations in membrane flux and/or selectivity restrict many applications of this technology.[1] The most common method for increasing flux is to decrease membrane thickness, and thus commercial membranes are generally prepared with a thin selective skin on a porous support that provides mechanical strength.[2,3] Methods for forming thin membrane skins include phase inversion,[4,5] interfacial polymerization,[6] plasma grafting,[7,8] casting,[9] and even deposition of films from the air/water interface.[10] Despite the success of these methods, synthesizing ultrathin, selective membranes is an ongoing challenge.

Multilayer polyelectrolyte films (MPFs) are potentially attractive materials for synthetic membrane skins because of their convenient synthesis and versatility. Synthesis of these films, first demonstrated by Decher and co-workers,[11,12] simply involves sequential adsorption of polycations and polyanions on an initially charged surface. The layer-by-layer deposition procedure affords control over film thickness on the nanometer scale, and the minimal total thickness of these films should allow high flux through polyelectrolyte multilayers deposited on highly permeable supports. Moreover, the selectivity of polyelectrolyte membranes may be tailored through selection of constituent polyelectrolytes as well as postdeposition cross-linking of films.[13] Applications of polyelectrolyte membranes recently explored by several research groups include gas separations,[14−17] selective pervaporation from water/organic solvent mixtures,[18,19] and ion separations.[13,20,21]

This paper focuses on understanding and controlling ion flux through multilayer polyelectrolyte membranes (MPMs) via control of the composition of these films. In previous studies of ion transport through MPMs,[13,20,21] fluxes of monovalent ions were higher than those of divalent ions. Krasemann and Tieke suggested that Donnan exclusion resulting from fixed charge in the membrane is responsible for this selectivity.[21] If Donnan exclusion is the dominant factor in effecting ion-transport selectivity in MPMs, then introduction of more net fixed charge into these membranes should lead to higher monovalent/divalent ion-transport selectivities. The purpose of this work is to explore the relationship between ion-transport selectivity and net fixed-charge density in MPMs. In the subsequent paper,[22] we show that templating with Cu^{2+} also provides a convenient method for introducing net fixed charge and can yield Cl^-/SO_4^{2-} selectivities as high as 600.

Although MPFs form due to electrostatic interactions, in the bulk of the film, charges on polycations are electrically compensated by charges on polyanions, and vice versa.[23,24] Schlenoff demonstrated that introduction of net fixed charge into MPFs requires postdeposition modification,[23] and several studies showed that MPFs can be modified after deposition to alter properties such as conductivity[25,26] or stability.[27,28] We chose to use partially derivatized poly(acrylic acid) (PAA) and poly(allylamine hydrochloride) (PAH) chains as model constituents for controlling charge in MPFs. To introduce net charge into films, we partially derivatized PAA and PAH with photolabile 2-nitrobenzyl (NB) and 2-nitrobenzyloxycarbonyl (NBOC) groups (Scheme 1). The underivatized $-COO^-$ groups in PAA and $-NH_3^+$ groups in PAH still allow for film formation through electrostatic adsorption, while UV irradiation of derivatized PAA/PAH films cleaves ester or carbamate bonds and liberates free acid or amine groups. These groups can then protonate/deprotonate to yield net negative (or positive) fixed charges in membranes (Figure 1). The newly formed charges are not electrically compensated by adjacent polyions but by oppositely charged ions from solution.[23] With the introduction of net fixed charge into the membrane, Donnan exclusion should be more pronounced, and monovalent/divalent ion transport selectivity should increase.

* To whom correspondence should be addressed. Phone 517-355-9715 x237; Fax 517-353-1793; e-mail bruening@cem.msu.edu.

10.1021/ma011633g CCC: $22.00
Published on Web 03/09/2002

Scheme 1

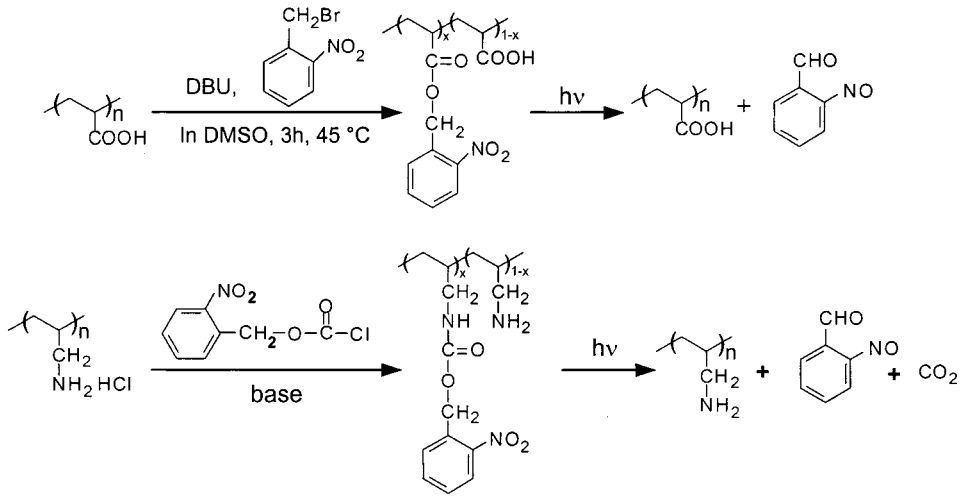

In principle, the simplest way to control net fixed charge in PAA/PAH membranes is to vary the pH of deposition solutions. Rubner showed that deposition of PAA/PAH films at low pH and subsequent immersion in higher pH solutions create ion-exchange sites in the film.[29] However, when we attempted depositing PAA/PAH membranes at pH 2.5 and running transport experiments at pH 5−6, we did not observe any increase in selectivity relative to PAA/PAH membranes prepared at pH 5.0. The use of deposition pH to control fixed charge could result in morphological changes in film structure that decrease selectivity.[30,31]

In contrast, introduction of fixed charge using photocleavable groups increases the selectivity of PAA/PAH films by an order of magnitude. The use of derivatization with photocleavable groups also allows knowledge of and control over the net, fixed charge in the membrane. Thus, by changing the extent of derivatization, one can control charge density and, hence, tailor ion-transport selectivity. With an estimate of charge density obtained from the extent of derivatization, we utilized a simple model to simulate ion transport through these membranes. The model suggests that both Donnan exclusion and selective diffusion play important roles in effecting selective transport.

Experimental Section

Materials. PAA (M_v = 450 000), PAH (M_w = 70 000), 2-nitrobenzyl bromide (99%), 2-nitrobenzyl alcohol (99%), phosgene solution (~20% in toluene), 1,8-diazabicyclo[5.4.0]-undec-7-ene (DBU, 98%), and dimethyl sulfoxide (DMSO, reagent) were purchased from Aldrich and used as received. Nitrobenzyl chloroformate was synthesized according to a literature procedure.[32] Deionized water (18 MΩ·cm, Milli-Q) was used in preparation of aqueous solutions. Membrane supports (Whatman Anodisc membrane filters with a nominal surface pore diameter of 0.02 μm) were purchased from Thomas Scientific.

Synthesis of 2-Nitrobenzyl-Derivatized PAA (NBPAA). PAA (720 mg, 10 mmol with respect to the repeating unit) was dissolved in 20 mL of DMSO (sonicate for 1 h, stir for 2 h at 45 °C to get complete dissolution), and DBU (1.52 g, 10 mmol, in 5 mL of DMSO) was added dropwise to this solution while stirring. 1.51 g (7 mmol) of 2-nitrobenzyl bromide was then added. The mixture was stirred at 45 °C for 3 h, after which 1 mL of acetic acid was added to neutralize DBU, and the solution was stirred for an additional 15 min. Derivatized polymer was then precipitated upon dropwise addition of the mixture into 1500 mL of pH 3 water. The precipitate was collected by filtration, washed thoroughly in water while stirring, and again collected by filtration. The polymer was dried under vacuum at 60 °C for 48 h, and 1.1 g of polymer was obtained (78% yield). ^{1}H NMR (*d*-DMSO as solvent) showed that ~50% of the −COOH groups in PAA were derivatized by NB groups (Figure 1, Supporting Information). The 23% and 65% NB-derivatized PAA were synthesized in a similar way (56% and 84% yield), except that the quantity of 2-nitrobenzyl bromide added was 0.86 g (4 mmol) and 1.73 g (8 mmol) for 23% and 65% derivatization, respectively. 23% NBPAA was precipitated into and washed with ethyl acetate-saturated pH 3 water.

Synthesis of 2-Nitrobenzyloxycarbonyl-Derivatized PAH (NBPAH). PAH (1.55 g, 17 mmol with respect to the repeating unit) was dissolved in 100 mL of water, and the solution was placed in an ice bath. After adjusting the pH of the solution to 3.0 with HCl, 1.84 g (8.5 mmol) of 2-nitrobenzylchloroformate in 5 mL of dry THF was added dropwise to the solution over a 2 h period while maintaining the solution pH between 3 and 4 through addition of 1 M NaOH. The reaction was then allowed to proceed at room temperature for another 2 h at pH 4. The suspension was collected by centrifugation. The polymer was redissolved in DMSO, precipitated upon addition to a 20% ethyl acetate/80% 2-propanol (v/v) mixture, and dried under vacuum at 50 °C for 72 h to yield 1.77 g of product (71% yield). ^{1}H NMR showed that ~50% of the amine groups in PAH were derivatized (Figure 1, Supporting Information).

Film Synthesis and Characterization. Before synthesizing MPMs on porous alumina supports, we prepared films on Al-coated wafers (200 nm of Al sputtered on Si(100)) to determine the optimum conditions for deposition. The Al wafer was UV/ozone cleaned for 15 min before immersion in a solution containing a polyanion (PAA or NBPAA). After a 10 min immersion, the wafer was rinsed with water for 1 min, immersed in a solution containing a polycation (PAH or NBPAH) for 10 min, and rinsed with water for 1 min to form the first bilayer. This procedure was repeated until the desired number of bilayers was deposited. (Drying with N_2 occurred only after deposition of the entire film.) The solutions used to form films were PAA (0.01 M, pH 5.0), PAH (0.02 M, pH 5.0), NBPAA (200 mg in 20 mL of DMSO + 80 mL of MeOH + 80 mg of KOH), and NBPAH (0.1 mM, pH 5.0). Concentrations of polymers are given with respect to the repeating unit, and pH values were adjusted with 0.1 M HCl or 0.1 M NaOH. Film thickness was measured with a rotating analyzer ellipsometer (J. A. Woollam model M-44), assuming a film refractive index of 1.5. Reflectance FTIR spectra were obtained with a Nicolet Magna-560 FTIR spectrometer using a Pike grazing angle attachment (80° angle of incidence). The spectrometer employs a MCT detector. Films were also deposited on porous alumina using the above procedure.

Photolysis. Polyelectrolyte films and membranes were irradiated in air with a medium-pressure mercury arc lamp

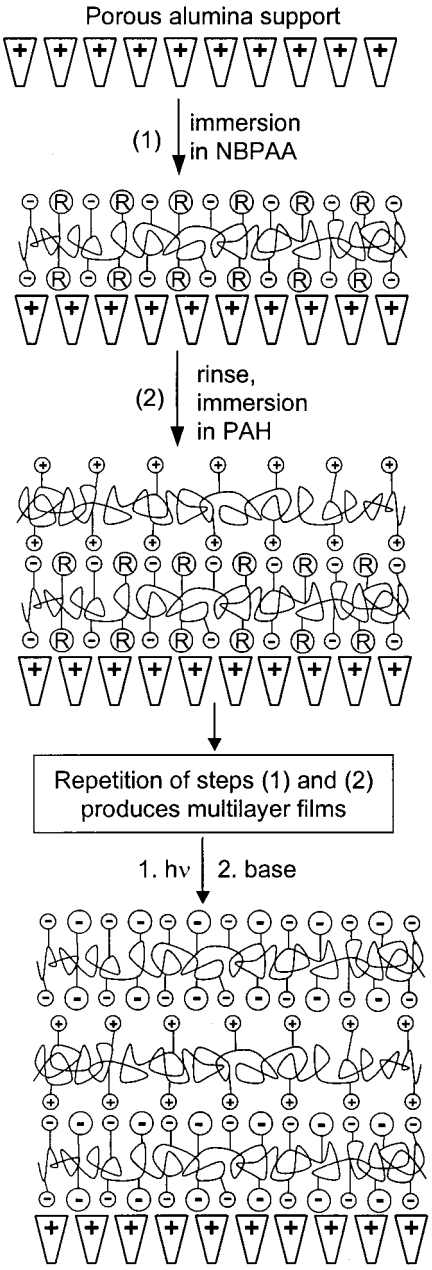

Figure 1. Schematic drawing of the formation of a multilayer polyelectrolyte membrane and subsequent introduction of net, fixed charge via photolysis. R represents the 2-nitrobenzyl (NB) photolabile functional group. Interweaving of layers is not shown for figure clarity.

(Hanovia, 450 W) without a filter at a distance of 30 cm from the source. The irradiation time was 60 min for all samples. Samples were dried with N_2 purging for 2 h before photolysis.

Transport Studies. The diffusion dialysis apparatus consists of two cells separated by the membrane, which is contained in the middle of a 2.5 cm long neck. The source cell was filled with 90 mL of a 0.1 M solution of the desired salt (NaCl, Na_2SO_4, or $MgCl_2$), while the receiving cell initially contained 90 mL of deionized water. The measured pH values of the unbuffered 0.1 M salt solutions were 5.3 (NaCl), 5.6 (Na_2SO_4), and 5.0 ($MgCl_2$). The area of the membrane exposed to the solution was 2 cm^2. The concentration of salt in the receiving cell was monitored at 5 min intervals for 45 min using a conductivity meter (Orion model 115). Solutions in both cells were vigorously stirred to minimize concentration polarization at the membrane surface. Membranes were soaked in water for at least 12 h before use, and three different membranes were prepared and tested for each type of film.

The conductivity in the receiving cell was transformed to concentration using a calibration curve. The flux (J) and selectivity (α) of ion transport were then calculated according to eqs 1 and 2

$$J = \frac{\Delta C}{\Delta t}\frac{V}{A} \tag{1}$$

$$\alpha_{1/2} = \frac{J_1}{J_2} \tag{2}$$

where $\Delta C/\Delta t$ is the concentration change with time calculated from the slope of a plot of concentration vs time, V is the volume of solution in the receiving cell, A is the exposed area of the membrane, and the subscripts 1 and 2 represent two different ions.

Results and Discussion

Derivatization of PAA and PAH. The 2-nitrobenzyl group and its analogues have been intensively employed as photoremovable protecting groups in a variety of synthetic strategies.[33,34] These photolabile groups were also, though less frequently, used to modify polymers.[35−37] Derivatization of PAA with 2-nitrobenzyl bromide occurs under mild conditions using a method developed by Nishikubo and co-workers for modification of poly(methacrylic acid).[35] Derivatization of PAH, however, is more challenging because both PAH and deprotonated poly(allylamine) are not very soluble in most organic solvents. To overcome this problem, we reacted PAH with 2-nitrobenzyl chloroformate in aqueous solution while controlling pH. This procedure is similar to the common practice in peptide synthesis of protecting amines with NBOC groups using an aqueous reaction.[34,38] Amines react with 2-nitrobenzyl chloroformate at a much faster rate than does water, and thus hydrolysis of 2-nitrobenzyl chloroformate is not a problem. In fact, at high pH, this reaction occurs so rapidly that polymer immediately begins to precipitate upon addition of nitrobenzyl chloroformate. To slow the reaction and achieve uniform derivatization without precipitation, we ran the reaction at a pH of about 4 so most of the amine groups would be protonated.[39]

Film Formation and Photochemistry. We prepared polyelectrolyte solutions in water in all cases where the polyelectrolyte was sufficiently soluble. Using a deposition pH of 5, we were able to obtain homogeneous films with reasonable thicknesses (Table 1).[29,40] NBPAH was only slightly soluble in water, but concentrations of 10^{-4} M were sufficient for film formation.[41] Derivatized PAA, however, did not dissolve in water, so we employed a DMSO/methanol cosolvent for these polymers and added a stoichiometric amount of KOH to deprotonate −COOH groups.[41−43] To assess whether changing deposition solvent affects film properties, we also prepared underivatized PAA/PAH films using PAA dissolved in DMSO/methanol that contained KOH. These films have basically the same IR spectra and ion-transport selectivities as films prepared only in water, but their thickness is ∼30% less than for the entirely water-based deposition. These experiments indicate that the enhanced selectivity (vide infra) of NBPAA/PAH membranes is not due to deposition from an organic solvent.

Figure 2 shows the reflectance FTIR spectra of a 10.5-bilayer 50% NBPAA/PAH film before and after UV irradiation. (The addition of an extra half bilayer results in NBPAA being the top layer in these films.) The strong

Table 1. Fluxes and Selectivities through Membranes Prepared from PAA, PAH, NBPAA, and NBPAH Deposited on Porous Alumina.

type of membrane[a,b]	film thickness (Å)[c]	flux ($\times 10^9$ mol/(cm^2 s))			selectivity[d]	
		NaCl	Na_2SO_4	$MgCl_2$	Cl^-/SO_4^{2-}	Na^+/Mg^{2+}
bare porous alumina		43 ± 2	32 ± 1	32 ± 1	1.3 ± 0.1	1.3 ± 0.1
PAA/PAH (10)	420 ± 16	22 ± 1	3.6 ± 0.3	1.9 ± 0.3	6.0 ± 0.8	12 ± 1
50% NBPAA/PAH (10)	260 ± 20	18 ± 1	0.15 ± 0.01	2.0 ± 0.1	120 ± 10	9.1 ± 0.5
PAA/50% NBPAH (10)	400 ± 35	14 ± 2	15 ± 1	0.35 ± 0.1	1.0 ± 0.1	43 ± 7
50% NBPAA/50% NBPAH (10)	320 ± 20	22 ± 2	1.8 ± 0.3	2.0 ± 0.2	12 ± 1	11 ± 1
PAA/PAH (10.5)	450 ± 30	20 ± 1	2.2 ± 0.2	2.1 ± 0.2	9.3 ± 0.6	10 ± 1
23% NBPAA/PAH (10.5)	330 ± 15	18 ± 2	0.19 ± 0.02	2.1 ± 0.2	100 ± 4	8.7 ± 0.1
50% NBPAA/PAH (10.5)	270 ± 15	16 ± 2	0.11 ± 0.02	2.0 ± 0.1	150 ± 10	8.1 ± 1.1
65% NBPAA/PAH (10.5)	275 ± 15	17 ± 2	0.10 ± 0.01	2.1 ± 0.2	170 ± 20	8.0 ± 0.7
PAA/50% NBPAH (10.5)	410 ± 35	15 ± 2	13 ± 1	0.4 ± 0.1	1.2 ± 0.1	38 ± 8

[a] The number in parentheses represents the number of bilayers deposited. [b] The percentage values represent the degree of derivatization of the particular polymer as calculated from NMR spectra. [c] Post-UV irradiation thickness of films prepared on Al-coated wafers. Thicknesses before irradiation were 10−25% higher. [d] Selectivities were calculated as the average of selectivity values from different membranes and not simply as a ratio of average flux values.

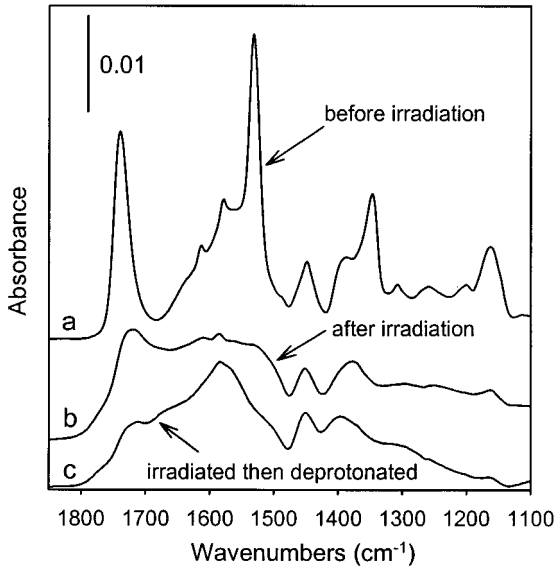

Figure 2. Reflectance FTIR spectra of a 10.5-bilayer 50% NBPAA/PAH film on an Al-coated wafer before (a) and after (b) UV irradiation. Spectrum (c) is that of the irradiated film after a 30 min immersion in pH 9.2 buffer solution and rinsing with ethanol.

absorbance at 1740 cm^{-1} is primarily due to the ester carbonyl groups of derivatized PAA, but underivatized, protonated −COOH groups likely also contribute to this peak. After 60 min of UV irradiation, peaks due to $-NO_2$ groups (1530 and 1345 cm^{-1}) completely disappeared, showing that photolysis was complete. The peak at 1720 cm^{-1} after irradiation is due largely to −COOH groups produced by photolysis (Scheme 1) and thus decreases significantly (∼60%) after deprotonation in pH 9.2 buffer. We also see an increased $-COO^-$ absorbance at 1575 cm^{-1} after deprotonation. Similar results were obtained for PAA/50% NBPAH films (Figure 2, Supporting Information). The carbamate carbonyl absorbance at 1716 cm^{-1} and peaks due to $-NO_2$ groups vanished after 60 min of UV irradiation, indicating complete photolysis. The mechanism of photocleavage of NB or NBOC groups proceeds via an intramolecular pathway,[36,38,44,45] and thus it is efficient in solid films as well as in solution.

Ion-Transport Studies. Table 1 summarizes fluxes and selectivities for several salts in diffusion dialysis experiments with PAA/PAH and derivatized PAA/PAH membranes. The table shows three interesting trends for 10.5-bilayer membranes: (1) photolyzed NBPAA/PAH membranes have 10−20-fold higher Cl^-/SO_4^{2-} selectivities than corresponding underivatized PAA/PAH membranes, (2) Cl^-/SO_4^{2-} selectivity for photolyzed 10.5-bilayer NBPAA/PAH membranes increases with the extent of derivatization, and (3) photolyzed PAA/NBPAH membranes show increased cation selectivities compared to PAA/PAH membranes (3−4 times) and minimal anion selectivities. NaCl fluxes are about the same for all coated membranes. Thus, high selectivity can be achieved without a significant decrease in flux.

As Figure 1 schematically shows, the difference between underivatized PAA/PAH membranes and UV-irradiated NBPAA/PAH membranes is that the latter contain net, fixed negative charge in the bulk of the film. Photolysis may also increase net charge at the surface of these films. Higher percentages of PAA derivatization lead to more negative fixed charge in membranes and hence higher anion-transport selectivity. Similarly, the introduction of net positive charges using photolyzed PAA/NBPAH increases Donnan exclusion of cations and hence monovalent/divalent cation-transport selectivity. However, this selectivity enhancement is not as significant as that displayed for anions by NBPAA/PAH membranes. A possible reason for the lower enhancement may be incomplete conversion of carbamates to amines during photocleavage. Although, removal of the nitrobenzyloxycarbonyl group is quantitative, side reactions may result in lower yields of amines. Patchornik and coworkers reported a 25% yield of amines when photocleaving nitrobenzyloxycarbonyl-protected amino acids.[38] This may also explain why the Cl^-/SO_4^{2-} selectivity of 10-bilayer 50% NBPAA/50% NBPAH membranes is twice as large as that of 10-bilayer PAA/PAH membranes. If derivatized PAH introduces less charge than does derivatized PAA, 50% NBPAA/50% NBPAH membranes would have a net negative charge and hence an increased Cl^-/SO_4^{2-} selectivity relative to PAA/PAH.

Because Donnan exclusion can result from charges at both the surface and the interior of a film, changing the outer layer of a membrane from a polyanion to a polycation should affect selectivity.[13,20,23,41] Table 1 shows some effect of changing the sign of surface charge, but the change in selectivity is not very large. Capping a membrane with a PAA or NBPAA top layer (10.5 bilayer membranes) increases anion selectivity by 20−50%, while capping with PAH (or NBPAH) (10 bilayer membranes) may slightly increase cation selectivity. In previous studies, however, Cl^-/SO_4^{2-} selectivity in-

Table 2. Estimated Charge Densities, Diffusion Coefficients, Donnan Selectivities, and Diffusional Selectivities for Derivatized PAA/PAH Membranes

membrane	23%NBPAA/PAH		50%NBPAA/PAH		65%NBPAA/PAH		PAA/50%NBPA	
Z_xC_x (M)	−1.8		−4.0		−4.6		1.0[b]	
D ($\times 10^{10}$ cm^2/s)	Cl^-	SO_4^{2-}	Cl^-	SO_4^{2-}	Cl^-	SO_4^{2-}	Na^+	Mg^{2+}
	130	5	200	12	260	15	65	3.5
α_D[a]	27		17		17		19	
α_E[a]	3.7		8.8		10		2.3	

[a] See eq 8 in the Appendix for the definition of α_D and α_E. [b] To obtain fixed charge density in this film, the initial estimate of amine concentration was divided by 4 to reflect a low yield of amine groups from photocleavage (reference 38).

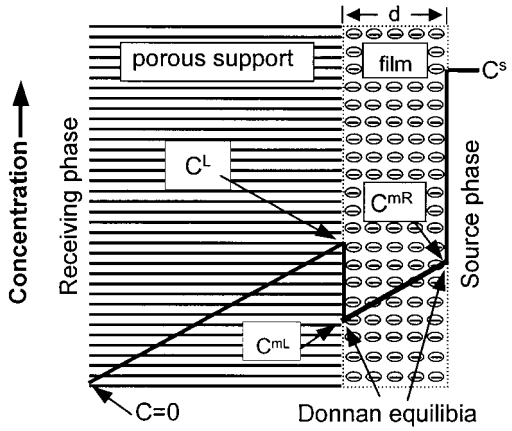

Figure 3. Schematic diagram of a model for ion transport through a multilayer polyelectrolyte membrane. The black lines represent the concentration profile (not to scale) of the ion that is excluded by the MPM. Symbols are defined in the Appendix.

creased by as much as 2 orders of magnitude when the outer layer of the film was a polyanion rather than a polycation.[13] The reason for the small effect in the present case is probably that films were prepared in the absence of supporting electrolyte. Preparation under these conditions reduces the net charge on the membrane surface,[23,46,47] and hence the bulk of the membrane will play a much larger role in determining selectivity.

Modeling of Ion Transport. To estimate the contributions of Donnan exclusion and selective diffusion to ion-transport selectivity, we utilized a simple model for ion transport based on previous simulations of ion-exchange membranes[48,49] and MPMs.[21,50] The model includes Donnan equilibria at the feed/membrane interface and at the alumina/polyelectrolyte film boundary (Figure 3) as well as Nernst−Planck transport within the membrane. Figure 3 portrays qualitatively the concentration profile in the membrane. We did not include a charged surface layer because reversing the charge in the top layer of the membrane had only a small effect on selectivity. To calculate diffusion coefficients in the membrane, we performed the procedure given in the Appendix.

The transport model requires a knowledge of the charge density, C_x, in MPMs. For our calculation, we assumed that all fixed charges resulted from photolysis of NBPAA or NBPAH. Pure PAA contains ~16 M −COOH groups. Assuming an equal volume fraction for PAA and PAH components and considering 50% derivatization, the concentration of net charge in 50% NBPAA/PAH films would be approximately 4 M. With this estimation, we calculated diffusion coefficients in different membranes along with values for diffusion, α_D, and electrostatic (Donnan), α_E, selectivities. The results are listed in Table 2.

Calculations with this simple model suggest that ion-transport selectivity is only partially due to Donnan exclusion and that diffusive selectivity is a larger factor than Donnan exclusion. However, the contribution of Donnan exclusion to selectivity does increase with increasing charge density in the membrane as would be expected. Diffusive selectivity is consistent with the fact that the calculated diffusion coefficients (ranging from 5.2×10^{-10} to 2.5×10^{-8} cm^2/s) in MPFs are very small.

The slow diffusion and the differences in Cl^- and SO_4^{2-} diffusion coefficients could result from steric hindrance and/or electrostatic interactions. Farhat and Schlenoff suggest that transport through polyelectrolyte multilayers occurs by hopping of ions between transient ion-exchange sites.[47] Because more highly charged ions require more ion-exchange sites, their movement through MPMs may be slower than that of monovalent ions. Yeager reported that the diffusion coefficient of Cl^- could be as much as 14 times larger than that of SO_4^{2-} in perfluorinated carboxylate membranes.[51] Even for similarly charged ions such as Na^+ and Cs^+, diffusion coefficients can differ by up to a factor of 4 in Nafion membranes.[52] By modeling Donnan dialysis data for ion transport through cation-exchange membranes, Miyoshi obtained effective diffusion coefficients as low as 6.33×10^{-8} and 1.34×10^{-8} cm^2/s for Na^+ and Mg^{2+}, respectively.[53] Thus, the low diffusion coefficients and the diffusional selectivities resulting from these simple simulations are within reasonable limits.

The limitations of the ion-transport model must be kept in mind, however. The simulation does not consider activity coefficients and possible differences in solubilities of different ions in MPMs.[54,55] This could account for the fact that calculated diffusivity selectivities in derivatized membranes are about 2-fold larger than total selectivities for pure PAA/PAH membranes. Additionally, charge densities are only approximate. However, even with these limitations, the modeling results and data for transport through underivatized membranes suggest that Donnan exclusion is only partially responsible for selectivities. Future work on determining partition coefficients would be helpful for a better understanding of transport, but such studies will be challenging given the minimal thickness of MPFs.

Conclusions

Introduction of net, fixed charge into MPMs through derivatization and photolysis is straightforward and quantitatively controllable. The presence of ion-exchange sites in the membrane significantly increases ion-transport selectivities, and this increase correlates with the charge density introduced into the membrane. Simulations suggest that the enhancement of selectivity is due to both Donnan exclusion and diffusivity differences among ions. In addition, the methods for deriva-

tizing poly(acrylic acid) and poly(allylamine) may provide a general way to modify the properties of MPFs.

Acknowledgment. We acknowledge partial financial support from the U.S. Department of Energy Office of Basic Energy Sciences and the American Chemistry Society Petroleum Research Fund. We thank Dr. P. Wagner for allowing us to use the UV lamps in his laboratory.

Appendix

To calculate diffusion coefficients in MPMs, we applied the following procedure. The ion concentration on the left side of the porous support/polyelectrolyte membrane interface, C_i^L, was calculated using eq 3

$$C_i^L = \frac{J_{\text{coated}}}{J_{\text{bare}}} C_i^S \tag{3}$$

where J_{coated} and J_{bare} are fluxes through coated and bare porous alumina supports, respectively, and C_i^S is the concentration of ion in the source-phase solution (0.1 M). This equation assumes that ion concentrations in the receiving phase are negligible and that flux through the alumina is proportional to a linear concentration gradient. The concentration of excluded ion just inside the left end of the coated polyelectrolyte film (Figure 3), C^{mL}, was calculated assuming Donnan equilibrium. For a salt A_xB_y with counterion charge Z_A and excluded ion charge Z_B, C_B^{mL} can be expressed by eq 4

$$C_B^{mL} = C_B^L \left(- \frac{Z_B C_B^{mL} + Z_x C_x}{Z_A C_A^L} \right)^{Z_B/Z_A} \tag{4}$$

where Z_x and C_x are the sign and concentration of the fixed charge in the membrane.

Next, we employed the Nernst−Planck equation (5) to calculate the excluded ion concentration, C_B^{mR}, at the right side of the polyelectrolyte film.

$$J_i = -D_i \frac{\mathrm{d}C_i}{\mathrm{d}x} - \frac{Z_i F D_i C_i}{RT} \frac{\mathrm{d}\phi}{\mathrm{d}x} \tag{5}$$

In this equation, D is the diffusion constant, ϕ is the electrical potential, x is the distance in membrane, and F, R, and T are the Faraday constant, the gas constant, and the temperature, respectively. Subscript i indicates the ith ion. Because the concentration of the excluded ion in the membrane is low, the migration term in the Nernst−Planck equation is negligible compared to the diffusion term for this ion. Assuming constant flux, eq 5 for the excluded ion can then be simplified to eq 6

$$J_B = -D_B \left(\frac{C_B^{mR} - C_B^{mL}}{d} \right) \tag{6}$$

where d is the thickness of the polyelectrolyte film. Rearrangement of eq 6 allows calculation of C_B^{mR} once C_B^{mL} is calculated. Finally, using eq 7, the concentration of the excluded ion in the source phase, C_B^S, could be calculated.

$$C_B^S = C_B^{mR} \left(- \frac{Z_B C_B^{mR} + Z_x C_x}{Z_A C_A^S} \right)^{Z_B/Z_A} \tag{7}$$

We performed the entire calculation iteratively, using the experimental flux and varying the diffusion coefficient of the excluded ion until the calculated excluded ion concentration in the source phase matched that used experimentally (0.1 M). Selectivity for species 1 (e.g., Cl^-) over species 2 (e.g., SO_4^{2-}) is given by eq 8

$$\alpha_{B_1/B_2} = \frac{J_{B_1}}{J_{B_2}} = \frac{D_{B_1}}{D_{B_2}} \frac{\Delta C_{B_1}^m}{\Delta C_{B_2}^m} = \alpha_D \alpha_E \tag{8}$$

where $\Delta C_B^m = C_B^{mR} - C_B^{mL}$ (Figure 3), and α_D and α_E denote selectivities arising from selective diffusion of ions and electrostatic exclusion, respectively.

Supporting Information Available: ^{1}H NMR spectra of PAA and PAH that were 50% derivatized with 2-nitrobenzyl and 2-nitrobenzyloxycarbonyl groups, respectively, and FTIR spectra of a 10.5-bilayer PAA/50% NBPAH film. This material is available free of charge via the Internet at http://pubs.acs.org.

References and Notes

(1) Liu, C.; Martin, C. R. *Nature (London)* **1991**, *352*, 50−52.
(2) Kesting, R. E.; Fritzche, A. K. *Polymeric Gas Separation Membranes*; John Wiley & Sons: New York, 1993.
(3) Brandt, D. C.; Leitner, G. F.; Leitner, W. E. In *Reverse Osmosis Membrane Technology, Water, Chemistry, and Industrial Applications*; Amjad, Z., Ed.; Van Nostrand Reinhold: New York, 1993; pp 1−36.
(4) Niwa, M.; Kawakami, H.; Nagaoka, S.; Kanamori, T.; Shinbo, T. *J. Membr. Sci.* **2000**, *171*, 253−261.
(5) Shieh, J.-J.; Chung, T.-S. *Ind. Eng. Chem. Res.* **1999**, *38*, 2650−2658.
(6) Parthasarathy, A.; Brumlik, C. J.; Martin, C. R.; Collins, G. E. *J. Membr. Sci.* **1994**, *94*, 249−254.
(7) Chen, H.; Belfort, G. *J. Appl. Polym. Sci.* **1999**, *72*, 1699−1711.
(8) Kilduff, J. E.; Mattaraj, S.; Pieracci, J. P.; Belfort, G. *Desalination* **2000**, *132*, 133−142.
(9) Linder, C.; Kedem, O. *J. Membr. Sci.* **2001**, *181*, 39−56.
(10) Zhang, L.-H.; Hendel, R. A.; Cozzi, P. G.; Regen, S. L. *J. Am. Chem. Soc.* **1999**, *121*, 1621−1622.
(11) Decher, G.; Hong, J. D. *Macromol. Chem., Macromol. Symp.* **1991**, *46*, 321−327.
(12) Decher, G.; Hong, J. D. *Ber. Bunsen-Ges. Phys. Chem.* **1991**, *95*, 1430−1434.
(13) Stair, J. L.; Harris, J. J.; Bruening, M. L. *Chem. Mater.* **2001**, *13*, 2641−2648.
(14) Leväsalmi, J.-M.; McCarthy, T. J. *Macromolecules* **1997**, *30*, 1752−1757.
(15) Kotov, N. A.; Magonov, S.; Tropsha, E. *Chem. Mater.* **1998**, *10*, 886−895.
(16) Stroeve, P.; Vasquez, V.; Coelho, M. A. N.; Rabolt, J. F. *Thin Solid Films* **1996**, *284−285*, 708−712.
(17) Ackern, F. v.; Krasemann, L.; Tieke, B. *Thin Solid Films* **1998**, *327−329*, 762−766.
(18) Krasemann, L.; Toutianoush, A.; Tieke, B. *J. Membr. Sci.* **2001**, *181*, 221−228.
(19) Meier-Haack, J.; Lenk, W.; Lehmann, D.; Lunkwitz, K. *J. Membr. Sci.* **2001**, *184*, 233−243.
(20) Harris, J. J.; Stair, J. L.; Bruening, M. L. *Chem. Mater.* **2000**, *12*, 1941−1946.
(21) Krasemann, L.; Tieke, B. *Langmuir* **2000**, *16*, 287−290.
(22) Balachandra, A. M.; Dai, J.; Bruening, M. L. *Macromolecules* **2002**, *35*, 3171−3178.
(23) Schlenoff, J. B.; Ly, H.; Li, M. *J. Am. Chem. Soc.* **1998**, *120*, 7626−7634.
(24) Laurent, D.; Schlenoff, J. B. *Langmuir* **1997**, *13*, 1552−1557.
(25) Kotov, N. A.; Dekany, I.; Fendler, J. H. *Adv. Mater.* **1996**, *8*, 637−641.
(26) Joly, S.; Kane, R.; Radzilowski, L.; Wang, T.; Wu, A.; Cohen, R. E.; Thomas, E. L.; Rubner, M. F. *Langmuir* **2000**, *16*, 1354−1359.
(27) Harris, J. J.; DeRose, P. M.; Bruening, M. L. *J. Am. Chem. Soc.* **1999**, *121*, 1978−1979.
(28) Chen, J.; Huang, L.; Ying, L.; Luo, G.; Zhao, X.; Cao, W. *Langmuir* **1999**, *15*, 7208−7212.

(29) Yoo, D.; Shiratori, S. S.; Rubner, M. F. *Macromolecules* **1998**, *31*, 4309−4318.
(30) Mendelsohn, J. D.; Barret, C. J.; Chan, V. V.; Pal, A. J.; Mayes, A. M.; Rubner, M. F. *Langmuir* **2000**, *16*, 5017−5023.
(31) Fery, A.; Schöler, B.; Cassagneau, T.; Caruso, F. *Langmuir* **2001**, *17*, 3779−3783.
(32) Dyer, R. G.; Turnbull, K. D. *J. Org. Chem.* **1999**, *64*, 7988−7995.
(33) Pillai, V. N. R. In *Organic Photochemistry*; Padwa, A., Ed.; Marcel Dekker: New York, 1987; Vol. 9, pp 225−323.
(34) Corrie, J. E. T.; Trentham, D. R. In *Bioorganic Photochemistry*; Morrison, H., Ed.; John Wiley: New York, 1993; Vol. 2, pp 243−305.
(35) Nishikubo, T.; IIzawa, T.; Takahashi, A.; Shimokawa, T. *J. Polym. Sci., Part A: Polym. Chem.* **1990**, *28*, 105−117.
(36) Beecher, J. E.; Cameron, J. F.; Fréchet, J. M. J. *J. Mater. Chem.* **1992**, *2*, 811−816.
(37) Matuszczak, S.; Cameron, J. F.; Fréchet, J. M. J.; Wilson, C. G. *J. Mater. Chem.* **1991**, *1*, 1045−1050.
(38) Patchornik, A.; Amit, B.; Woodward, R. B. *J. Am. Chem. Soc.* **1970**, *92*, 6333−6335.
(39) Yoshikawa, Y.; Matsuoka, H.; Ise, N. *Br. Polym. J.* **1986**, *18*, 242−246.
(40) Shiratori, S. S.; Rubner, M. F. *Macromolecules* **2000**, *33*, 4213−4219.
(41) Dubas, S. T.; Schlenoff, J. B. *Macromolecules* **1999**, *32*, 8153−8160.
(42) Dai, J.; Jensen, A. W.; Mohanty, D. K.; Erndt, J.; Bruening, M. L. *Langmuir* **2000**, *17*, 931−937.
(43) Cochin, D.; Passmann, M.; Wilbert, G.; Zentel, R.; Wischerhoff, E.; Laschewsky, A. *Macromolecules* **1997**, *30*, 4775−4779.
(44) DeMayo, P. *Adv. Org. Chem.* **1960**, *2*, 367−425.
(45) Gravel, D.; Giasson, R.; Blanchet, D.; Yip, R. W.; Sharma, D. K. *Can. J. Chem.* **1991**, *69*, 1193−1200.
(46) Schlenoff, J. B.; Dubas, S. T. *Macromolecules* **2001**, *34*, 592−598.
(47) Farhat, T. R.; Schlenoff, J. B. *Langmuir* **2001**, *17*, 1184−1192.
(48) Meyer, K. H.; Sievers, J.-F. *Helv. Chim. Acta* **1936**, *19*, 649−664.
(49) Teorell, T. In *Progress in Biophysics and Biophysical Chemistry*; Butler, J. A. V., Randall, J. T., Eds.; Academic Press: New York, 1953; Vol. 3, pp 305−369.
(50) Lebedev, K.; Ramirez, P.; Mafé, S.; Pellicer, J. *Langmuir* **2000**, *16*, 9941−9943.
(51) Herrera, A.; Yeager, H. L. *J. Electrochem. Soc.* **1987**, *134*, 2446−2451.
(52) Rollet, A.-L.; Simonin, J.-P.; Turq, P. *Phys. Chem. Chem. Phys.* **2000**, *2*, 1029−1034.
(53) Miyoshi, H. *J. Membr. Sci.* **1998**, *141*, 101−110.
(54) Makino, K.; Oshima, H.; Kondo, T. *Colloid Polym. Sci.* **1987**, *265*, 911−915.
(55) Paula, S.; Volkov, A. A.; Deamer, D. W. *Biophys. J.* **1998**, *74*, 319−329.

MA011633G